

## Superionicity in the hydrogen storage material $\text{Li}_2\text{NH}$ : Molecular dynamics simulations

C. Moysés Araújo,<sup>1,\*</sup> Andreas Blomqvist,<sup>1</sup> Ralph H. Scheicher,<sup>1</sup> Ping Chen,<sup>2,3</sup> and Rajeev Ahuja<sup>1,4</sup>

<sup>1</sup>*Department of Physics and Materials Science, Condensed Matter Theory Group, Uppsala University, P.O. Box 530, SE-751 21 Uppsala, Sweden*

<sup>2</sup>*Department of Physics and Department of Chemistry, National University of Singapore, 117542 Singapore, Singapore*

<sup>3</sup>*Dalian Institute of Chemical Physics, Dalian 116023, People's Republic of China*

<sup>4</sup>*Department of Materials and Engineering, Applied Materials Physics, Royal Institute of Technology (KTH), SE-100 44 Stockholm, Sweden*

(Received 19 January 2009; revised manuscript received 6 March 2009; published 8 May 2009)

We have employed *ab initio* molecular dynamics simulations in an attempt to study a temperature-induced order-disorder structural phase transformation that occurs in  $\text{Li}_2\text{NH}$  at about 385 K. A structural phase transition was observed by us in the temperature range 300–400 K, in good agreement with experiment. This transition is associated with a melting of the cation sublattice ( $\text{Li}^+$ ), giving rise to a superionic phase, which in turn is accompanied by an order-disorder transition of the N-H bond orientation. The results obtained here can contribute to a better understanding of the hydrogen storage reactions involving  $\text{Li}_2\text{NH}$  and furthermore broaden its possible technological applications toward batteries and fuel cells.

DOI: [10.1103/PhysRevB.79.172101](https://doi.org/10.1103/PhysRevB.79.172101)

PACS number(s): 61.20.Gy, 61.20.Ja, 71.15.Pd, 71.15.Mb

Superionic solids form a class of materials of great importance for applications in renewable energy technologies such as electrolytes in fuel cells and batteries.<sup>1</sup> Special attention has been given to those materials which have Li atoms as the highly mobile entities, as for instance in  $\text{Li}_3\text{N}$ .<sup>2</sup> This compound has also been discussed as a promising hydrogen storage medium<sup>3–9</sup> since it was demonstrated by Chen *et al.*<sup>10</sup> that upon hydrogenation, it transforms into lithium imide ( $\text{Li}_2\text{NH}$ ) plus lithium hydride ( $\text{LiH}$ ), facilitating the storage of a large amount of hydrogen in a reversible process. These findings have subsequently prompted a flurry of investigations both from experimentalists and theorists on  $\text{Li}_2\text{NH}$ , a compound which had been known since the 1950s.<sup>11</sup> This material undergoes an order-disorder transition at around 400 K and a vivid discussion has taken place in the literature about its correct low- and high-temperature structure.<sup>12–19</sup> Here we intend to focus on other important questions which arise, such as: how do the ion transport properties change as  $\text{Li}_3\text{N}$  is hydrogenated (i.e., in the  $\text{Li}_2\text{NH}$  phase)? Can the order-disorder transition in this phase enhance the ionic conductivity? What would be the mobile species in the imide compound?

The high Li conductivity is expected to be significantly diminished in  $\text{Li}_2\text{NH}$  as compared to that in  $\text{Li}_3\text{N}$  due to strong electrostatic interaction with the partially positively charged hydrogen atoms in the  $\text{NH}_2^-$  units. However, based on first-principles molecular dynamics (MD) simulations, we reveal in this work that the order-disorder transition at around 400 K actually involves the dissolution of the previously frozen Li sublattice into a superionic phase with  $\text{Li}^+$  cations diffusing through channels formed by the solid  $\text{NH}_2^-$ -anion sublattice. Time-averaged, such a scenario would be indistinguishable from the experimentally observed simple-cubic Li sublattice. The intriguing findings of our study may broaden the possible technological applications of  $\text{Li}_2\text{NH}$ .

In our MD simulations, forces were calculated from density-functional theory<sup>20</sup> as implemented in the (VASP) code.<sup>21,22</sup> The calculations are based on the generalized gra-

dient approximation (GGA) (Ref. 23) and made use of the projector-augmented wave (PAW) approach.<sup>24</sup> A  $1096 \text{ \AA}^3$  supercell was constructed containing 128 atoms from the high-temperature phase antifluorite structure (space-group  $Fm\bar{3}m$ ) with H atoms randomly distributed on  $48h$  sites. This structure has been used as the initial configuration in our MD simulations for all simulated temperatures, but we have also tested how the system evolves if other choices for the starting structure are considered. The results of these tests showed that even at the lowest simulated temperature the system always equilibrates within less than 10 ps to the same configuration and thus shows no signs of memory effects to the initial structure. This behavior is likely due to electrostatic forces playing the main role in the atomic rearrangement.

We have used a cutoff energy of 700 eV which was found to be required in order to reach convergence in the total energy. The valence states used were  $2s$  for Li,  $2s2p$  for N, and  $1s$  for H. Inclusion of the Li  $1s$ -semicore states in the valence was tested by us, but it did not lead to any significant changes in the results presented here. The large dimensions of the supercell allowed us to limit sampling of the Brillouin zone to the  $\Gamma$  point. The simulations were performed in the canonical ensemble (volume, particle number, and temperature are fixed).<sup>25</sup> The velocities were rescaled after every third time step to set the kinetic energy of the system to a specific value. In between the rescaling steps, the microcanonical (NVE) ensemble was employed. This approach is deemed to be the most suitable one to treat a material which is rich in light elements such as hydrogen, without being forced to use extremely short-time steps. We were thus able to employ time steps corresponding to 1 femtosecond (fs) and each simulation was allowed to run for a total of 20 000 time steps. To ensure that any memory of the initial configuration is completely erased, the first 10 000 time steps were reserved for equilibrating the system and were discarded from the subsequent analysis. We then proceeded to extract and analyze the pair-distribution functions, the

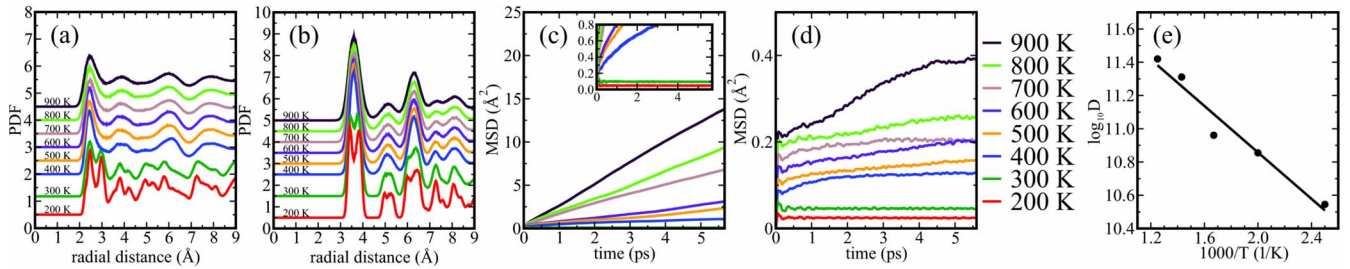


FIG. 1. (Color online) Pair-distribution function for (a) Li-Li and (b) N-N pairs in the temperature range of 200–900 K. Mean-square displacement for (c) Li and (d) N ions in the temperature range of 200–900 K. The inset for (c) shows the Li data for 200 and 300 K in greater detail. (Grayscale: the ordering of the curves in panels (a)–(d) always follows the same pattern with 200 K at the bottom, 100 K increments for adjacent curves, and 900 K at the top.) (e) Arrhenius plot of the Li diffusion coefficients (where  $D$  is in units of  $\text{\AA}^2/\text{s}$ ).

mean-square displacements, and the bond-orientation distributions.

To begin the discussion of our results, we present the pair distribution functions (PDF) in Figs. 1(a) and 1(b). The PDF is a very suitable measure to analyze the structure of a material both in experiment and in theory. However, in our theoretical calculations, we can go even further and analyze the PDF for each pair of elements individually. This allows us to track more clearly which sublattices are involved in a particular transition. Here, we show the PDF in  $\text{Li}_2\text{NH}$  for Li-Li [Fig. 1(a)], and N-N [Fig. 1(b)] pairs for the range of temperatures  $T=200\text{--}900$  K. The former and latter provide information about the structures of cation and anion sublattices, respectively.

The most noticeable feature is that the Li-Li PDF curve undergoes a drastic change as the temperature reaches 400 K. The characteristic double-peak structure in the range 2.5–3.0  $\text{\AA}$  disappears and similarly the peaks for larger distances give way to a much smoother curve. The overall structure of the PDF then remains essentially unchanged as the temperature is further raised up to  $T=900$  K, with only a further broadening of the peaks taking place. The peak positions indicate that the Li ions prefer a simple-cubic arrangement for  $T>400$  K. However, as we will exemplify in the following, this configuration only corresponds to the time-averaged distribution of  $\text{Li}^+$  and a more detailed analysis reveals that a transition takes place at 400 K in which the Li sublattice undergoes a transition from solid to a “quasiliquid phase.” The latter term is meant to emphasize the difference to a regular liquid where atoms or clusters of atoms are continuously in a state of free diffusion (while still strongly interacting with each other). By contrast, Li ions in the “quasiliquid phase” are seen to spend the majority of time oscillating about their respective lattice sites, but possess sufficient mobility to also diffuse over to the adjacent lattice site when the conditions set by the immediate surrounding are favorable. Such diffusion events were found by us to occur very frequently for  $T>400$  K, and overall this behavior leads to an effective diffusion of Li ions through the entire system, as will become clear from further analysis below.

Let us now briefly discuss the N-N PDF curves shown in Fig. 1(b). The integration of the nearest-neighbor peak shows that each N atom is coordinated by 12 other N atoms, characteristic of the face-centered cubic (fcc) lattice. This nearest-neighbor peak is in fact composed of two subpeaks

which merge into one narrow peak at 400 K, indicating a transition from a distorted fcc lattice to an essentially perfect one. The positions and heights of the second and third peaks further confirm that N atoms occupy a fcc lattice in agreement with the experimental findings.<sup>12,14–16,18</sup>

Having analyzed the time-averaged positions and their internal relations, we now turn our attention to the diffusion of atoms in the system as the temperature is increased. The mean-square displacement (MSD) is plotted as a function of time in Figs. 1(c) and 1(d) for both the Li ions and the N ions. As can be seen from the flat MSD curve in Fig. 1(c), Li is restricted to small vibrations around its equilibrium lattice site for temperatures of 200 K and 300 K. However, once the temperature reaches 400 K, the MSD is clearly showing a finite slope, indicating diffusion of the Li ions in the system. The slope of the MSD curve, and hence the diffusion coefficient, continues to increase with rising temperature. Taken together with the high-temperature PDF results for Li in Fig. 1(a), this goes to show that the Li cation sublattice in  $\text{Li}_2\text{NH}$  undergoes a kind of melting transition around 400 K and then continues to stay in a “quasiliquid” state as the temperature rises further. Such a behavior would be hard to observe in x-ray diffraction experiments due to the small scattering cross section of Li, and it might instead appear in the measurement as if Li is located (on average) at the cubic lattice sites coinciding with the broad peaks in the PDF [Fig. 1(a)]. Indeed, a detailed analysis of our MD simulation for  $T \geq 400$  K revealed that the Li ions spend the majority of time at these cubic lattice points. However, the Li ions are clearly seen not to be restricted to these lattice points, but can rather diffuse from one lattice site to another. The frequency of these diffusion events increases quickly with temperature, as the rising slope of the MSD curves attests. One of the main criteria for the solid state is therefore no longer fulfilled, namely, that the Li ions are fixed to a rigid sublattice. Instead, their state is more accurately described as a “quasiliquid phase” in the sense defined above. From a fitting of the linear regime in the MSD curves the diffusion coefficients have been extracted for the various simulated temperatures. These are displayed in the Arrhenius plot in Fig. 1(e). The thus calculated activation energy of the superionic phase is 60 meV, in good agreement with the expected activation energy range of a superionic solid, which is typically tens of meV.<sup>26,27</sup>

The  $\text{Li}_2\text{NH}$  crystal as a whole is certainly not melting at a

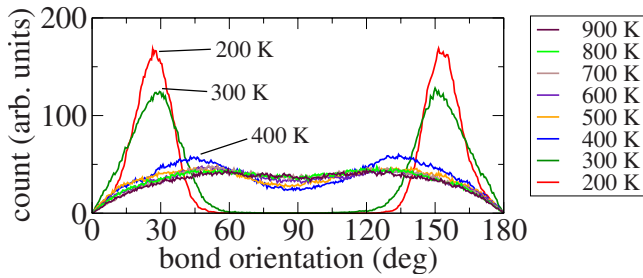


FIG. 2. (Color online) Bond-orientation distribution for N-H bonds in the temperature range of 200–900 K.

low temperature of 400 K and the retention of the solid state can clearly be seen in the behavior of the N ions. The corresponding MSD curve in Fig. 1(d) demonstrates that there is no significant diffusion of N ions until the temperature reaches values around 900 K. However, we do observe a slight deviation from a perfectly zero slope for  $T \geq 400$  K. As we will be able to explain in greater detail below, this behavior is related to an adjustment of the N sublattice, which is made possible by the more flexible distribution of the Li ions in their quasiliquid state. We also draw attention again to the mending of the double-peak structure of the nearest-neighbor N-N PDF peak into the single-peak structure [Fig. 1(b)] that prevails for temperatures above 400 K, highlighting the adjustment to a more regular N sublattice as well.

The onset of Li diffusion at  $T=400$  K coincides with the disordering of N-H bonds around the same temperature as can be seen from the bond-orientation distribution plot in Fig. 2. Here we plot the angle that the N-H bonds make with the  $z$  axis in the system. One can clearly see how the N-H bonds are initially fixed in direction at the low temperatures 200 and 300 K, making angles of about 30 and 150° with the  $z$  axis. For  $T \geq 400$  K, the N-H bonds start to spread out to a drastically broader distribution which becomes increasingly unrestricted as the temperature rises further.

The rearrangement of the N-H bonds and the diffusion of the Li ions are mutually fortifying. For low temperatures, the partially positively charged H atoms bound to N in  $\text{NH}_2^-$  have to orient in a particular way to minimize repulsion from nearby positively charged Li ions. This ordering of the low-temperature phase is removed when the Li ions become mobile which in turn allows a more flexible arrangement for the H atoms (while still being anchored to the fixed N ion sublattice). Vice versa, the freely rotating H atoms allow the diffusing Li ions to occupy (on average) lower-energy positions of a cubic lattice. It is difficult to say with certainty what is cause and effect here, the disordering of the N-H bond orientation or the mobility of  $\text{Li}^+$ . Their strong interdependence suggests that their onset coincides at around the same temperature between 300 and 400 K.

We observed the transition in the N-N PDF curve from a distorted fcc lattice to a more or less perfect fcc lattice [Fig. 1(b)]. This behavior can now be understood from the rotations of the partially positively charged H atoms which lead to a more isotropic charge distribution around the N ion. In return, the interaction with the environment (the diffusing Li ions) is no longer strongly direction dependent, allowing the

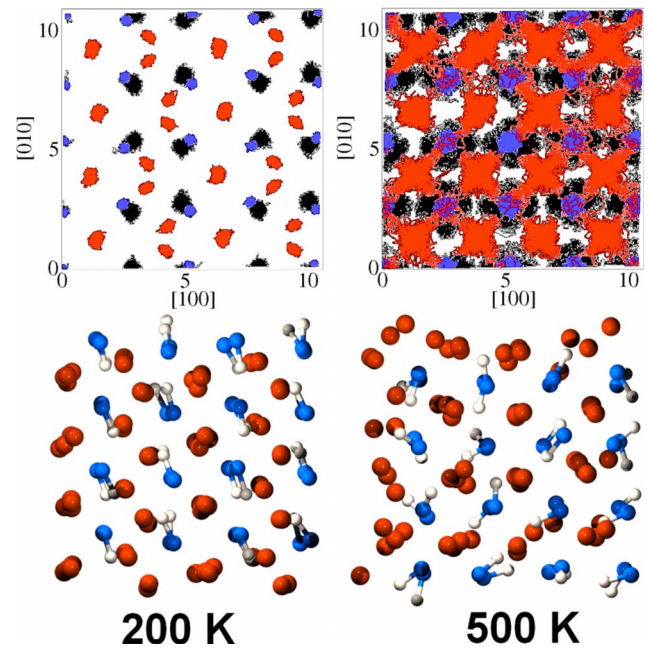


FIG. 3. (Color online) Top panel: ion trajectories projected into the  $x$ - $y$  for 200 and 500 K (cell dimensions are in units of Å). Bottom panel: 3D view of two frames from our MD simulations at 200 and 500 K. Both panels have Li shown in red (light gray) and N in blue (dark gray). H is shown in black (white) in the upper (lower) panel.

N ions to take on sites of the ideal fcc lattice.

Both x-ray and neutron-diffraction measurements yield time-averaged structures which makes it difficult to study ionic diffusion. MD simulations can follow the computed atomic trajectories of any element with the desired precision. Realistically, the amount of time that can be simulated without compromising accuracy is of course rather limited. Nevertheless, as we have shown here, it is possible to extract a sufficient amount of information to obtain new insights about the mechanisms of the temperature-induced phase transition in  $\text{Li}_2\text{NH}$ .

Our interpretation of the results based on the analysis of PDFs, MSD, and bond-orientation distribution can be further corroborated by visualizing the atomic positions in the MD simulations as a function of time. The trajectories shown in Fig. 3 help to illustrate how the ions are confined to their lattice sites for  $T < 400$  K and how Li becomes mobile for  $T > 400$  K. Furthermore, as an example, we also display typical configurations for  $T=200$  K and  $T=500$  K (Fig. 3). It can be seen that for the lower temperature, Li ions are only slightly displaced from their lattice sites which form a zigzag pattern. The N-H bonds show very strong ordering in their orientation. For higher temperatures, Li ions are seen to diffuse through the system while N ions continue to form a crystalline lattice. Particularly obvious is the disordering of the N-H bonds which exhibit no longer the former preferential orientation seen at lower temperatures.

In summary, we presented results from an extensive *ab initio* MD study of  $\text{Li}_2\text{NH}$  in the range  $T=200$ –900 K with the aim to understand the mechanism of a temperature-induced structural change in this material. The combined in-

formation from the mean-square displacement of the ions and the pair-distribution functions leads us to the conclusion that the sublattice formed by the  $\text{Li}^+$  cations undergoes a transition to a superionic solid state at around 400 K with the Li ions possessing sufficiently high mobility to diffuse within channels formed by the solid  $\text{NH}^{2-}$ -anion sublattice. This is simultaneously accompanied by a more random distribution of the N-H bonds. The activation energy in the superionic phase was found to be 60 meV, in good agreement with the expected activation energy.<sup>26,27</sup> Time-averaged, using, e.g., x-ray or neutron scattering, the Li sublattice would appear as the experimentally observed simple-cubic structure. In order to experimentally observe the superionic state, it would be beneficial if measurements of the ionic conductivity could be performed.

Likewise, the emergence of the liquid subphase of  $\text{Li}^+$  cations in  $\text{Li}_2\text{NH}$  could have important consequences for the interpretation of solid-solid reactions that occur not only in hydrogen-storage processes, and should be of great value in achieving a more accurate understanding of the systems involved in such reactions. Furthermore, this work also provides insights about the correlation between Li transport and the N-H bond rotational mobility in a system that could be of interest for battery-related issues and problems related to ionic transport in general.

We acknowledge support by STINT, VR, Futura, Göran Gustafsson Stiftelse, and Wenner-Gren Stiftelserna. SNIC and UPPMAX provided computing time.

---

\*Corresponding author; moyses.araujo@fysik.uu.se

- <sup>1</sup>P. Boolchand and W. J. Bresser, *Nature (London)* **410**, 1070 (2001).
- <sup>2</sup>P. P. Prosini, *J. Electrochem. Soc.* **150**, A1390 (2003).
- <sup>3</sup>M. S. Dresselhaus and I. L. Thomas, *Nature (London)* **414**, 332 (2001).
- <sup>4</sup>L. Schlapbach and A. Züttel, *Nature (London)* **414**, 353 (2001).
- <sup>5</sup>R. D. Cortright, R. R. Davda, and J. A. Dumesic, *Nature (London)* **418**, 964 (2002).
- <sup>6</sup>N. L. Rosi, J. Eckert, M. Eddaoudi, D. T. Vodak, J. Kim, M. O’Keeffe, and O. M. Yaghi, *Science* **300**, 1127 (2003).
- <sup>7</sup>J. S. Rigden, *Hydrogen: The Essential Element* (Harvard University Press, Cambridge, MA, 2003).
- <sup>8</sup>J. Alper, *Science* **299**, 1686 (2003).
- <sup>9</sup>W. Grochala and P. P. Edwards, *Chem. Rev.* **104**, 1283 (2004).
- <sup>10</sup>P. Chen, Z. Xiong, J. Luo, J. Lin, and K. L. Tan, *Nature (London)* **420**, 302 (2002).
- <sup>11</sup>R. Juza and K. Opp, *Z. Anorg. Allg. Chem.* **266**, 313 (1951).
- <sup>12</sup>T. Ichikawa, N. Hanada, S. Isobe, H. Leng, and H. Fujii, *J. Phys. Chem. B* **108**, 7887 (2004).
- <sup>13</sup>K. Miwa, N. Ohba, S. I. Towata, Y. Nakamori, and S. I. Orimo, *Phys. Rev. B* **71**, 195109 (2005).
- <sup>14</sup>J. F. Herbst and L. G. Hector, Jr., *Phys. Rev. B* **72**, 125120 (2005).
- <sup>15</sup>T. Noritake, H. Nozaki, M. Aoki, S. Towata, G. Kitahara, Y. Nakamori, and S. Orimo, *J. Alloys Compd.* **393**, 264 (2005).
- <sup>16</sup>K. Ohoyama, Y. Nakamori, S. Orimo, and K. Yamada, *J. Phys. Soc. Jpn.* **74**, 483 (2005).
- <sup>17</sup>B. Magyari-Köpe, V. Ozolinš, C. Wolverton, *Phys. Rev. B* **73**, 220101(R) (2006).
- <sup>18</sup>M. P. Balogh, C. Y. Jones, J. F. Herbst, Jr, L. G. Hector and M. Kundrat, *J. Alloys Compd.* **420**, 326 (2006).
- <sup>19</sup>T. Mueller and G. Ceder, *Phys. Rev. B* **74**, 134104 (2006).
- <sup>20</sup>W. Kohn and L. J. Sham, *Phys. Rev.* **140**, A1133 (1965).
- <sup>21</sup>G. Kresse and J. Furthmüller, *Comput. Mater. Sci.* **6**, 15 (1996).
- <sup>22</sup>G. Kresse and D. Joubert, *Phys. Rev. B* **59**, 1758 (1999).
- <sup>23</sup>J. P. Perdew and Y. Wang, *Phys. Rev. B* **45**, 13244 (1992).
- <sup>24</sup>P. E. Blöchl, *Phys. Rev. B* **50**, 17953 (1994).
- <sup>25</sup>A fixed particle density entails a  $T$ -dependent pressure in the system. The pressure increases almost linearly with  $T$  from  $-3.4$  to  $-0.14$  GPa. Predicting the eventual pressure in a canonical ensemble calculation before the simulation run is difficult.
- <sup>26</sup>C. H. J. Stuhmann, H. Kreiterling, and K. Funke, *Solid State Ionics* **154-155**, 109 (2002).
- <sup>27</sup>J. B. Goodenough, in *Solid State Electrochemistry*, edited by P. G. Bruce (Cambridge University Press, New York, 1995), pp. 48–52.